

# Quantitative Theory of Surface Tension and Surface Potential of Aqueous Solutions of Electrolytes

Vladislav S. Markin<sup>\*,†</sup> and Alexander G. Volkov<sup>‡</sup>

Department of Anesthesiology, UT Southwestern Medical Center, Dallas, Texas 75390-9068, and  
Department of Chemistry, Oakwood College, Huntsville, Alabama 35896

Received: June 3, 2002

The surface tension and surface potential of aqueous solutions of inorganic electrolytes are calculated. The new model includes image forces at liquid interfaces, ions of finite radii, the hydrophobic effect, and the Parsons–Zobel effect. For the first time, a good correlation between theory and experimental data both qualitatively and quantitatively is obtained for different inorganic salts over a wide range of concentrations.

## Introduction

Mechanical and electrical properties of all interfaces, from pure water to elaborate surfaces of cellular membranes, depend on ion adsorption at these surfaces. This phenomenon plays a very important role in colloid and physical chemistry, biology, and medicine. The structure and stability of large biomolecules and membranes depends on the distribution of counterions in the aqueous phase. The transport of ions through ion channels in cellular membranes is determined by the surface potential generated by adsorption of ions from aqueous phase. Conduction of nerve impulses and the effect of anesthetics strongly depend on this adsorption. Therefore, it is very important to know the structure of aqueous interfaces and distribution of ions in them.

Other fields in which this knowledge is indispensable are environmental aquatic chemistry and chemistry of the atmosphere. Chemical reactions involving aerosolized particles in the atmosphere are derived from the interaction of gaseous species with the liquid water associated with aerosol particles and with dissolved electrolytes. For example, the generation of HONO from nitrogen oxides takes place at the air/water interface in seawater aerosols or in clouds. Clouds convert between 50 and 80% of SO<sub>2</sub> to H<sub>2</sub>SO<sub>4</sub> which contributes to the formation of acid rain.<sup>1</sup> Another example is the release of chlorine atoms from sea salt aerosols reacting with the gaseous components. Molecular chlorine, a photolabile precursor of Cl atoms, is a product arising from a heterogeneous reaction of ozone with Cl<sup>−</sup> ions. Measurements of inorganic chlorine gases indicate the presence of reactive chlorine in the remote marine boundary layer; reactions involving chlorine and bromine can affect the concentrations of ozone, hydrocarbons, and cloud condensation nuclei. The heterogeneous reaction between HOBr and HCl converts significant amounts of inactive chlorine (HCl) into reactive chlorine (ClO). These are only a few examples of global processes in environmental chemistry occurring at the air/water interface.

In all these cases, the adsorption of simple inorganic ions is especially interesting. In the beginning of the last century, Heydeweller<sup>2</sup> found that surface tension of water increases with addition of inorganic electrolytes having relatively small ions. Some organic molecules (sodium formate, glycine, amino acids at the isoelectric point when both the amino and the carboxyl groups are ionized in the form of zwitterion) also increase

surface tension. The surface tension of solutions increases almost linearly with increasing concentration of salts, and for inorganic salts there is an empirical equation:  $\gamma = \gamma_0 + bc$ , where  $b = 1.7 \text{ mN m}^{-1} \text{ M}^{-1}$  for LiOH,  $1.8 \text{ mN m}^{-1} \text{ M}^{-1}$  for NaOH and KOH,<sup>3</sup>  $1.63 \text{ mN m}^{-1} \text{ M}^{-1}$  for NaCl, and  $1.33 \text{ mN m}^{-1} \text{ M}^{-1}$  for KCl.<sup>4</sup> For organic tetraalkylammonium salts the constant  $b$  decreases with increasing of cation radius: for tetramethylammonium chloride  $b$  is positive, for tetraethylammonium chloride  $k$  is about zero, and for bigger cations  $b$  is positive.<sup>3</sup>

This phenomenon was explained as a result of negative adsorption of small ions. Wagner<sup>5</sup> was the first to describe this phenomenon as an electrostatic effect of image forces. Onsager and Samaras<sup>6</sup> derived equations, which predicted the increase of surface tension with an increase of electrolyte concentration, but only for the very dilute solutions. Later Buff and Stillinger<sup>7</sup> presented the statistical mechanical formulation of the same problem by also employing the conventional model for very dilute solutions. They calculated the molecular distribution functions from a generalized form of Kirkwood's integral equation and found the surface tension directly from the molecular theory for this thermodynamic parameter. These approaches were quite successful, although they used a simple theory for point charges and did not take into account effects of ion radii. It was Frumkin<sup>8,9</sup> who indicated that the increase of surface tension and surface potential of aqueous solutions of inorganic salts depended on ionic radii. However, it was believed for a long time that equivalent concentrations of different salts gave very similar variations of surface tension,<sup>10</sup> at least at small concentrations. Later it was found that the differences are rather pronounced even at small concentrations.<sup>11</sup> At higher concentrations, different ions exhibit specific differences: the higher the ion hydration, the higher the surface tension increment. The contributions of two ions of the electrolyte to the surface tension appear almost additive.

There was a series of attempts to advance the theoretical explanation of the surface tension given by Onsager and Samaras,<sup>6</sup> but without much success. A critical discussion of these attempts can be found in Randles.<sup>12</sup> Krylov and Levich<sup>13</sup> considered the discreteness of the charge of adsorbed ions but found this effect to be rather small. An interesting paper was recently published by Levin<sup>14</sup> who, in contrast to Onsager and Samaras, explored another route to surface tension. Levin<sup>14</sup> identified the excess surface tension directly from the Helmholtz free energy necessary to create an interface. That permitted improvement of the agreement between theory and experiment at higher concentrations.

\* Corresponding author. Tel: 214-648-5632. Fax: 214-648-6532. E-mail: Vladislav.Markin@UTSOUTHWESTERN.edu.

<sup>†</sup> UT Southwestern Medical Center.

<sup>‡</sup> Oakwood College.

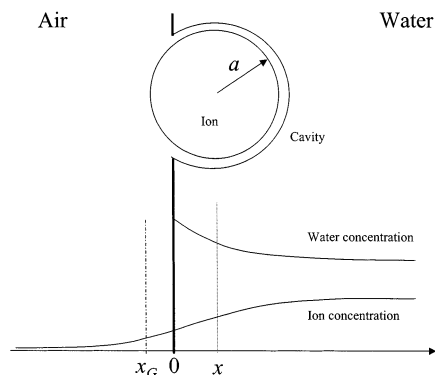


**Figure 1.** Distribution of water and ion concentration at distance  $x$  from the air/water interface;  $x_G$  is the position of the Gibbs dividing surface.

Having in mind all these improvements, we still have to stress that the original works of Wagner<sup>5</sup> and Onsager and Samaras<sup>6</sup> correctly identified the major players determining the surface tension of the aqueous electrolyte: image forces at the interface and negative adsorption of ions. Using the well-known Gibbs adsorption equation, they<sup>5,6</sup> calculated the value of surface tension without ascribing too much importance to the difference between anions and cations.

The surface tension increment was explained at least for the small concentration of electrolytes. In contrast to this, the situation with the surface potential was completely hopeless. In the Onsager–Samaras approach,<sup>6</sup> if there is no difference between anions and cations (beyond the charge sign), there is no reason to expect that they would generate any surface potential because they would equally be negatively adsorbed at the interface and their charges completely compensate each other. Therefore the whole effect of change of the surface potential of water in the presence of electrolytes originates from the difference between anions and cations. In this sense, this effect is more subtle and elusive than surface tension. Therefore it comes as no surprise that up to now there was no satisfactory theoretical explanation of this phenomenon.

The explanation of the surface potential can be found in the difference in ionic radii and their manifestations at the water surface. Because of finite radii, different ions can interact differently with interfaces.<sup>15,16</sup> This results in a different interfacial distribution of energy, concentration, and charge density of these ions. We shall use the model of ions with finite radii to describe both surface tension and surface potential at the wide range of concentrations.

### Theoretical

**The Model: Ions of Finite Radii at the Air/Water Interface.** Let us consider an air/water interface as depicted in Figure 1. Coordinate  $x$  is directed from the interface to the bulk of water.

The energy of an ion with radius  $a$  at the interface was calculated by Kharkats and Ulstrup.<sup>15,16</sup> They accounted for the Born solvation energy and the energy of interaction with the image. When  $x > a$ , the energy of an ion can be presented as

$$W_{\text{KU}}(x) = \frac{(ze_0)^2}{32\pi\epsilon_0\epsilon_{\text{W}}a} \left\{ 4 + \left( \frac{\epsilon_{\text{W}} - \epsilon_{\text{A}}}{\epsilon_{\text{W}} + \epsilon_{\text{A}}} \right) \frac{2a}{x} + \left( \frac{\epsilon_{\text{W}} - \epsilon_{\text{A}}}{\epsilon_{\text{W}} + \epsilon_{\text{A}}} \right)^2 \times \left[ \frac{2}{1 - (2x/a)^2} + \frac{a}{2x} \ln \frac{2x+a}{2x-a} \right] \right\} \quad (1)$$

The first term in parentheses in (1) represents the Born solvation energy, and the last two terms give the interaction with the image.

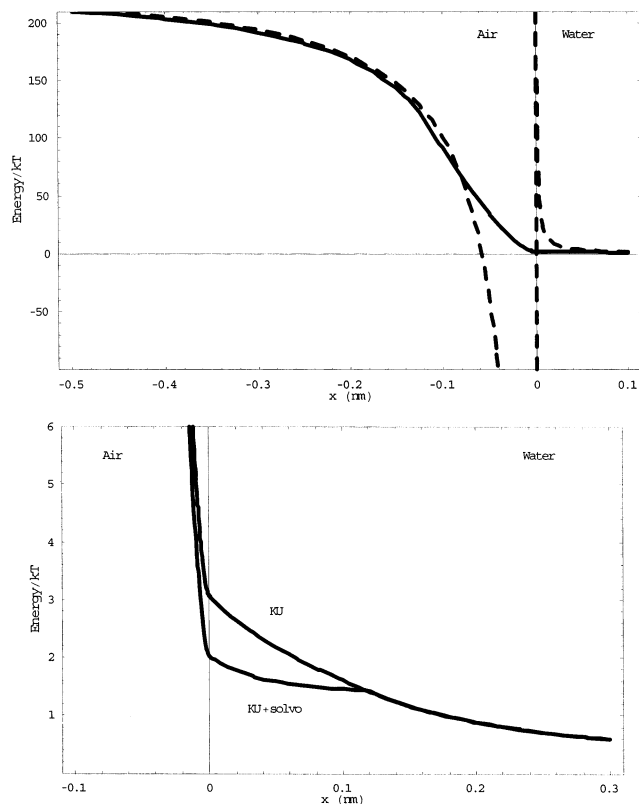


**Figure 2.** Energy of ions in different models. The air/water interface is positioned at  $x = 0$ . (A) Dependence of the image energy on the distance from the air/water interface for  $\text{Na}^+$  (solid line) and for a point charge (dashed line). (B) Dependence of the image (KU) and sum of solvophobic and image (KU + solv) energies on the distance from the air/water interface for a sodium ion at low concentration.

In the region  $0 \leq x \leq a$ :

$$W_{\text{KU}}(x) = \frac{(ze_0)^2}{32\pi\epsilon_0\epsilon_{\text{W}}a} \left\{ \left( 2 + \frac{2x}{a} \right) + \left( \frac{\epsilon_{\text{W}} - \epsilon_{\text{A}}}{\epsilon_{\text{W}} + \epsilon_{\text{A}}} \right) \left( 4 - \frac{2x}{a} \right) + \left( \frac{\epsilon_{\text{W}} - \epsilon_{\text{A}}}{\epsilon_{\text{W}} + \epsilon_{\text{A}}} \right)^2 \left[ \frac{(1 + x/a)(1 - 2x/a)}{1 + 2x/a} + \frac{a}{2x} \ln \left( 1 + \frac{2x}{a} \right) \right] \right\} + \frac{(ze_0)^2}{16\pi\epsilon_0\epsilon_{\text{A}}a} \left( \frac{2\epsilon_{\text{A}}}{\epsilon_{\text{W}} + \epsilon_{\text{A}}} \right)^2 \left( 1 - \frac{x}{a} \right) \quad (2)$$

When the center of the ion is right at the interface ( $x = 0$ ), the electrostatic Gibbs energy is equal to

$$W_{\text{KU}}(x=0) = \frac{(ze_0)^2}{4\pi\epsilon_0(\epsilon_{\text{W}} + \epsilon_{\text{A}})a} \quad (3)$$

When the ion is located in the air, the electrostatic free energy is obtained from (1) and (2) by exchanging  $\epsilon_{\text{W}} \leftrightarrow \epsilon_{\text{A}}$ . The Kharkats–Ulstrup equations have recently become rather popular, but unfortunately in a number of references they were distorted by a series of typographic errors beginning with the authors' original paper of 1991.<sup>15</sup> Recently Wu et al.<sup>17</sup> pointed to these mistakes but failed to give correct expressions and added their own errors to these equations. The reader should be careful when considering these different references. The correct version can be found in Benjamin<sup>18</sup> or in Volkov et al.<sup>19</sup>

The image energy can be derived from eqs 1–3 by subtracting the Born energy  $W_{\text{Born}} = W_{\text{KU}}(+\infty)$ . This energy for a sodium ion is presented in Figure 2 by the solid line; the dashed line gives the image energy of a point charge. One can see an

important difference: the energy of a point charge becomes infinite at the interface, whereas the Kharkats–Ulstrup function eliminates this feature and makes the curve continuous.

Equations 1 and 2 give the energy of a lone ion interacting only with its image. However, the presence of other ions in the solution will modify this interaction due to Debye screening of electrical field. Therefore the ion/image interaction should decay much faster than in eqs 1 and 2. To take this effect into consideration, we shall introduce the screening function  $f(x)$  as follows:

$$f(x) = \begin{cases} 1 & \text{if } x \leq a_{\text{an.}} + a_{\text{cat.}} \\ \exp[-2\kappa(x - a_{\text{an.}} - a_{\text{cat.}})] & \text{if } x > a_{\text{an.}} + a_{\text{cat.}} \end{cases} \quad (4)$$

with Debye constant  $\kappa$  and ion radii  $a_{\text{an.}}$  and  $a_{\text{cat.}}$ . For binary electrolyte the Debye constant is given by  $\kappa = \sqrt{e_0^2 c_0 / \epsilon_0 \epsilon k T \sum_i z_i^2}$ . This definition consistently takes into consideration the model of ions as hard spheres so that cations (cat) and anions (an) cannot approach each other closer than at  $a_{\text{an.}} + a_{\text{cat.}}$ . Therefore the image energy can be presented as

$$W_{\text{image}}(x) = f(x)[W_{\text{KU}}(x) - W_{\text{KU}}(\infty)] \quad (5)$$

This function would work rather well for calculations of the surface tension. However, for calculation of the surface potential one would need to take into account more subtle effects that help to distinguish between cations and anions. One of them is the solvophobic effect that takes into consideration the work of creating the cavity to place the ion into the solvent (see ref 19 and references therein). If one assumes that there is surface tension  $\gamma_{\text{cavity}}$  in this cavity, then in the bulk of the solvent the solvophobic energy is  $4\pi a^2 \gamma_{\text{cavity}}$ . If the ion crosses the interface from right to left (Figure 1), the area of the cavity decreases and with it the solvophobic energy. If the ion center is positioned at  $x$ , then in the range  $-a \leq x \leq a$  the energy is  $2\pi a(a + x) \gamma_{\text{cavity}}$ ; at  $x < -a$ , it is 0. If the reference point is selected in the bulk of water, then these quantities should be decreased by  $4\pi a^2 \gamma_{\text{cavity}}$  and one finally obtains the relative solvophobic energy as

$$W_{\text{solvophobic}} = -2\pi a \gamma_{\text{cavity}} \begin{cases} 2a & \text{if } x < -a \\ a - x & \text{if } -a \leq x \leq a \\ 0 & \text{if } x > a \end{cases} \quad (6)$$

The surface tension in the cavity is not very well-known; it is believed to be close to the surface tension of water but is probably less than that, due to the small radius of curvature as was argued by Tolman.<sup>20</sup> We shall estimate this value in the range 40–50 mN/m. Both components of the energy (image and solvophobic) are presented in Figure 2B for sodium ions at a low electrolyte concentration. One can see that the solvophobic effect decreases the energy at the interface.

The total energy of ion  $i$  with charge number  $z_i$  includes image and solvophobic components and electrical potential of the electrical double layer  $\varphi(x)$ :

$$W_i(x) = W_{\text{image}}(x) + W_{\text{solvophobic}}(x) + z_i e_0 [\varphi(x) - \varphi(\infty)] \quad (7)$$

Notice that the image energy and the solvophobic energy also depend on the type of ions.

To calculate the spatial distribution of ions we used standard methods for the electrical double layer. The Poisson–Boltzmann

equation can be presented<sup>19</sup> in the following way:

$$\frac{d^2 \varphi}{dx^2} = - \frac{e_0 c_0}{\epsilon_0 \epsilon} \sum_i z_i \exp \left[ - \frac{W_i(x)}{kT} \right] \quad (8)$$

where dielectric constant  $\epsilon$  assumes the value  $\epsilon_A$  or  $\epsilon_W$  depending on coordinate  $x$ . We assume that the aqueous phase contains a binary 1:1 electrolyte with bulk concentration  $c_0$ . Energy  $W_i$  is given by eq 7, and the summation includes both cations and anions. For boundary conditions, we assume that the electrical potential  $\varphi$  and its gradient  $\nabla \varphi$  in the bulk are zero:

$$\varphi(\infty) = 0 \quad \left. \frac{d\varphi}{dx} \right|_{\infty} = 0 \quad (9)$$

Equation 8 with boundary conditions (9) will be solved numerically and both surface tension and surface potential will be found.

**Concentration Dependence of Surface Tension.** In the first theoretical description of the surface tension of electrolyte solutions Wagner<sup>5</sup> and Onsager and Samaras<sup>6</sup> presented the energy of interaction of an ion with its image at the distance  $x$  from the interface as

$$W(x) = \frac{e_0^2}{16\pi\epsilon_0\epsilon_W x} \exp(-2\kappa x) \quad (10)$$

where  $e_0$  designates the charge of the ion,  $\epsilon_0$  is the permittivity of free space,  $\epsilon_W$  is the dielectric constant of water, and  $\kappa$  is Debye constant. This function is presented in Figure 2A by the dashed line. The surface excess of ions ( $i$ ) with respect to water ( $W$ ) was calculated as

$$\Gamma_{i(W)} = c_0 \int_0^\infty \{ \exp[-w(x)/kT] - 1 \} dx \quad (11)$$

Using the surface excesses of ions, Onsager and Samaras calculated the surface tension as a sum of a series and tabulated this sum. For very dilute solutions of 1:1 electrolytes, they found an analytical expression for the surface tension, which they called the limiting law:

$$\Delta\gamma = \gamma - \gamma_0 = 1.012c \log(1.467/c) \quad (12)$$

This equation is presented in Figure 3 (dashed line), together with experimental data for NaCl. As one can see, the limiting law coincides with the experimental data only at concentrations smaller than 0.1 M, after which the discrepancy becomes very large. The tabulated values improve the situation only a little. And of course, the limiting law does not distinguish between different ions describing them by the same equation.

The main drawback of previous approaches was the absence of an appropriate model of ions at the air–water interface. To obtain a radical improvement of the theory of surface tension in the presence of simple electrolytes, we shall use the new expression for energy (7) that accounts for both finite radius of ions and solvophobic effect.

We shall begin with calculation of the surface tension, because the surface potential at low electrolyte concentrations has some peculiarities and cannot be found directly from the standard Poisson–Boltzmann equation. Fortunately, this does not influence the calculation of surface tension, because at low concentrations the potential is small and has no effect on the distribution of ions that are determined by image forces and solvophobic effect only.

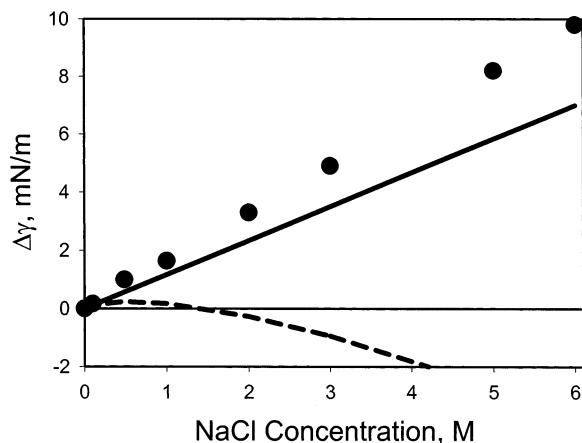


**Figure 3.** Surface tension of water in the presence of NaCl: (dots) experimental data;<sup>4</sup> (dashed line) Onsager limiting law; (solid line) present work.

Let us calculate surface excesses of ions  $i$ , with respect to water  $\Gamma_{i(W)}$ . The Gibbs dividing surface corresponding to zero-excess of water ( $\Gamma_W = 0$ ) does not necessarily coincide with the surface of water as demonstrated in Figure 1, where its coordinate is designated  $x_G$ . If the bulk concentration of ions in the air and water are correspondingly 0 and  $c_0$ , then the ion surface excesses are

$$\Gamma_{i(W)} = c_0 \int_{-\infty}^{x_G} \exp\left[-\frac{W_i(x)}{kT}\right] dx + c_0 \int_{x_G}^{+\infty} \left\{ \exp\left[-\frac{W_i(x)}{kT}\right] - 1 \right\} dx \quad (13)$$

The position of the Gibbs dividing surface  $x_G$  was found in the following manner. Water concentration in solutions of simple salts depends virtually linearly on salt concentration, as one can see in Figure 4 for solutions of NaCl and KCl. The data for these examples were taken from the *CRC Handbook of Chemistry and Physics*.<sup>4</sup>

The trend lines of these dependences can be presented as

$$c_W = 55.6 - \alpha c_{\text{salt}} \quad (14)$$

The slope  $\alpha$  was found for NaCl to be equal to 1.18 and for KCl equal to 1.73.

One has to have in mind that at the far right end of the concentrations scale (about 3 M) the data taken from the *CRC Handbook of Chemistry and Physics*<sup>4</sup> probably are not very reliable because of the saturation effect. However, at smaller concentrations, the data ideally fit a straight line and this is the only result we take from these data. Besides, as indicated later in the text, the effect of the displacement of the Gibbs dividing surface is rather small. Therefore, any small inaccuracy resulting from the saturation effect will become negligible in the final result.

Because concentrations of anions and cations are slightly different at the interface, we shall define the salt concentration as the mean of the two. Then the spatial distribution of water concentration in the solution can be presented by

$$c_W(x) = 55.6 - \frac{\alpha c_0}{2} \left\{ \exp\left[-\frac{W_{\text{anion}}(x)}{kT}\right] + \exp\left[-\frac{W_{\text{cation}}(x)}{kT}\right] \right\} \quad (15)$$

Assuming that the actual surface of water is located at coordinate

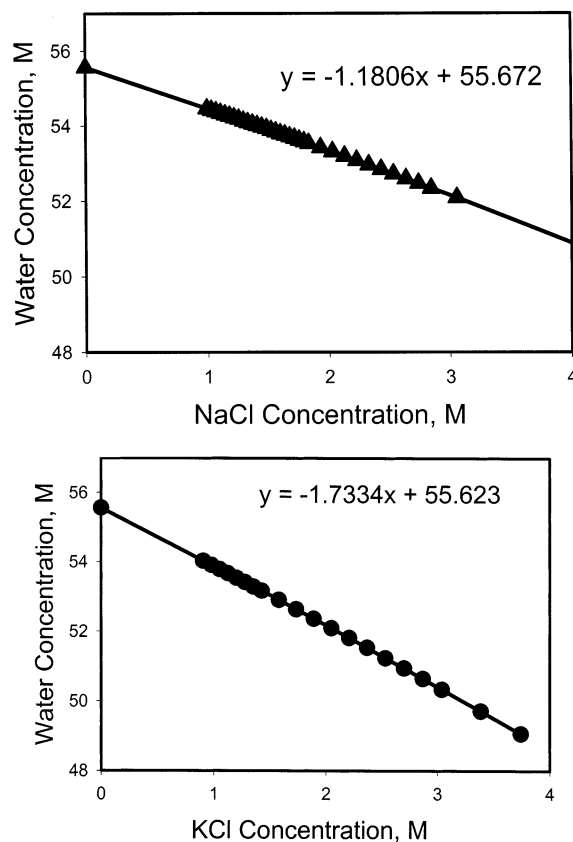


**Figure 4.** Water concentration in aqueous solutions of NaCl (A) and KCl (B). Experimental points are taken from ref 4.

$x_D = 0$ , the water excess at this dividing surface is

$$\Gamma_{W(x_D=0)} = \frac{c_0}{2} \int_0^{\infty} \left\{ 2 - \exp\left[-\frac{W_{\text{anion}}(x)}{kT}\right] + \exp\left[-\frac{W_{\text{cation}}(x)}{kT}\right] \right\} dx \quad (16)$$

and the position of the dividing surface corresponding to zero water excess is

$$x_G = \frac{c_0}{2(55.6 - \alpha c_0)} \int_0^{\infty} \left\{ 2 - \exp\left[-\frac{W_{\text{anion}}(x)}{kT}\right] + \exp\left[-\frac{W_{\text{cation}}(x)}{kT}\right] \right\} dx \quad (17)$$

However, the position of this Gibbs dividing surface is different from 0 only at very high salt concentrations.

In the isothermal case the surface tension is related to the surface excesses by the Gibbs adsorption equation

$$d\gamma = - \sum_{i=1}^2 \Gamma_{i(W)} d\mu_i \quad (18)$$

In the simple case of a uni-univalent electrolyte the increment of the surface tension can be presented as

$$\Delta\gamma = \gamma - \gamma_0 - \int_0^c (\Gamma_{\text{anion}(W)} + \Gamma_{\text{cation}(W)}) \frac{dc}{c} \quad (19)$$

To calculate this quantity, we have to solve the Poisson–Boltzmann equation (11) and find the integral in eq 19. We carried out numerical integration for a number of different



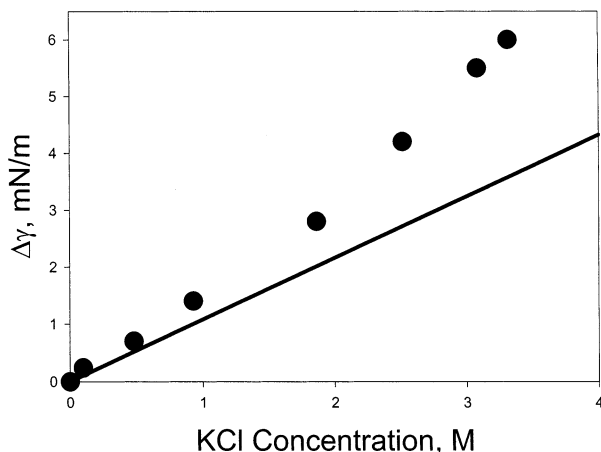


**Figure 5.** Dependence of the surface tension of aqueous solution of KCl on concentration. Experimental points are taken from ref 4. The solid line is calculated using eq 19.

electrolytes and compared them with experimental data. Results for NaCl are presented in Figure 3 and for KCl in Figure 5. In these calculations we used the following values of ion radii according Gourary and Adrian:<sup>21</sup>  $a_{\text{Na}} = 0.117$  nm,  $a_{\text{K}} = 0.149$  nm,  $a_{\text{Cl}} = 0.164$  nm. The surface tension in the cavities for anions and cations was taken as the same and equal to  $\gamma_{\text{cavity}} = 50$  mN m<sup>-1</sup>. One can see that the present model provides radical improvement comparative to the Onsager limiting law, although at very high concentrations there is a certain discrepancy between experimental and theoretical data. Notice that quantitative difference between NaCl and KCl is rather small, and this will not be so for the surface potential.

**Surface Potential.** The elegant theory by Onsager and Samaras<sup>6</sup> for surface tension predicted a zero surface potential because it did not envision any difference between the way cations and anions interacted with the interface. However, experimental observations clearly demonstrated rather pronounced surface potential depending on electrolyte concentration. The sign of this potential with respect to the bulk of water very often is negative, although some salts give positive potential.

In the absence of a rigorous theory, a number of semiempirical attempts were made (see refs 12 and 22 and references therein). The increase of the surface tension with electrolyte concentration was interpreted as the presence of a solute-free layer 4–5 Å thick at the surface. Randles<sup>22</sup> assumed that this surface layer is completely inaccessible to cations in solutions of all alkali metal salts, but anions can penetrate more closely to the surface. In other words, Randles postulated two different planes of closest approach for anions and cations. The anions built up negative charge at the surface that was balanced by positive charge of cations deeper in the bulk and hence a negative surface potential was established. Using this simple model and the standard kinetic theory of the electrical double layer, Randles calculated concentration dependence of the surface potential. However, comparing his theoretical results with experimental data he had to admit that his model was “quite unable to account for the observed surface potentials”. The problem was not simply in numbers: theoretical predictions were *qualitatively* wrong. The Randles theory predicted that the surface potential at low concentrations should increase as a square root of concentration, whereas experimentally this dependence was either linear or even superlinear. Therefore the theoretical and experimental lines had opposite curvature, which was unacceptable.

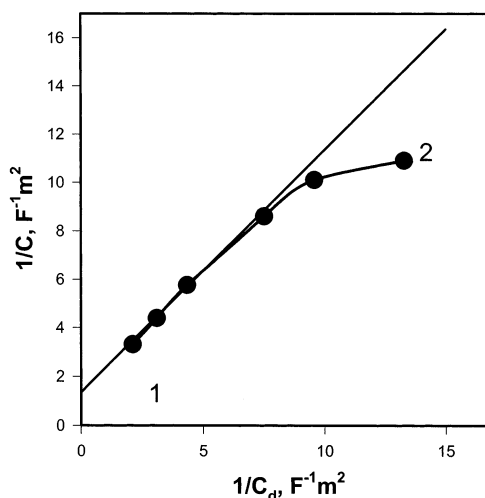


**Figure 6.** Parsons–Zobel (PZ) plots for the nitrobenzene/water interface. The solid line was calculated according to the Gouy–Chapman theory with the concentration independent capacitance of compact layer equal to 0.74 F/m<sup>2</sup>. Experimental points are taken from Samec et al.<sup>23</sup>

This finding seemed rather strange because the model qualitatively *cannot* be wrong: there is definitely spatial separation of positive and negative ions at the interface that creates surface charge, and this charge should be balanced by the other part of the electrical double layer. At low concentrations the electrical potential is small and does not influence the ion distribution at the interface. Therefore one can conclude that the surface charge  $Q$  should grow linearly with the electrolyte concentration:  $Q \sim c_0$ . If the double layer capacitance is  $C_{\text{DL}}$ , then the surface potential is  $\varphi = Q/C_{\text{DL}}$ . According to the Gouy–Chapman theory at low concentrations, the capacitance is equal to the capacitance  $C_{\text{diffuse}}$  of the diffuse part of the layer and hence is proportional to the square root of the electrolyte concentration:

$$C_{\text{DL}} \sim C_{\text{diffuse}} \sim \sqrt{c_0} \quad (20)$$

That is why Randles came up with the result

$$\varphi \sim \sqrt{c_0} \quad (21)$$

However, there is an interesting anomaly in the capacitance of the double electric layer: at low electrolyte concentrations it does not obey the theory of Gouy–Chapman. This phenomenon named the Parsons–Zobel effect was discovered by Samec et al.<sup>23</sup> and later studied by Wandlowski et al.<sup>24</sup> These authors analyzed the relationship between inverse capacitances  $C_{\text{DL}}^{-1}$  and  $C_{\text{diffuse}}^{-1}$ . According to Gouy–Chapman–Stern or Verwey–Nissen theory this relationship is given by a straight line with a cutoff at the ordinate determined by the compact layer capacitance.<sup>25</sup> However, experimentally observed, the total capacitance at low concentrations of electrolyte (large  $C_{\text{diffuse}}^{-1}$ ) strongly departs from the straight line and displays the tendency to become constant (Figure 6). We shall discuss this peculiarity later but now just accept this fact “at face value”.

If relationship (20) does not hold and the double layer capacitance is rather constant, then relationship (21) should rather transform to

$$\varphi \sim c_0 \quad (22)$$

This corresponds much better to the experimental observations.

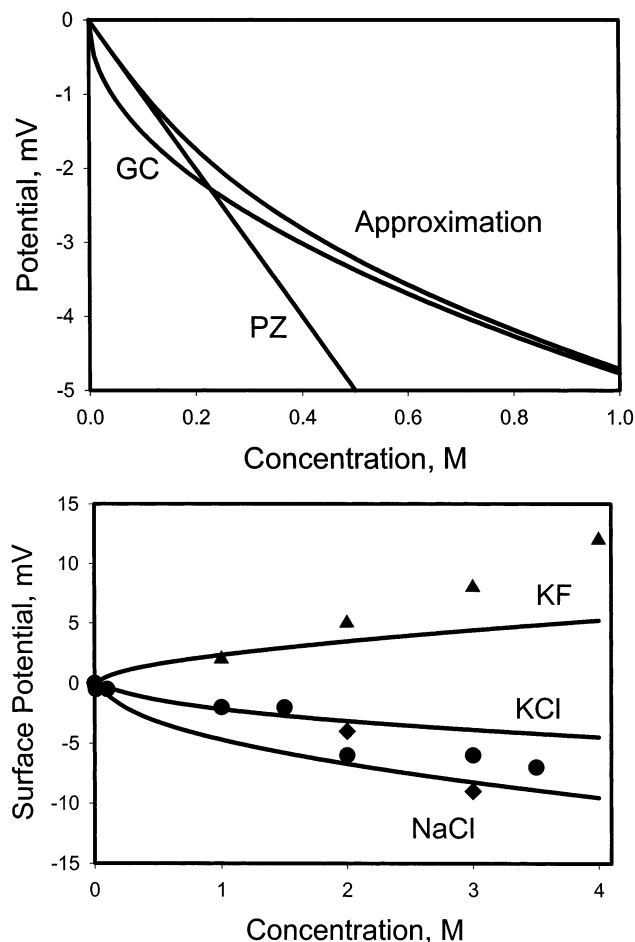


**Figure 7.** Dependence of the surface potential on concentration. (A) Theoretical estimations for NaCl aqueous solution based on the Gouy-Chapman (GC =  $-4.77\sqrt{c}$ ) model, with the Parsons-Zobel (PZ =  $-10c$ ) effect at liquid interfaces, and the actual curve (Approximation =  $x(0.0001 + 0.00193x^2)^{-1/4}$ ). (B) Theoretical lines for KF (triangles), KCl (filled circles), and NaCl (diamonds). Experimental points are taken from Frumkin<sup>8,9</sup> and Randles.<sup>12</sup> The curves were drawn according to the following equations: KF =  $[(2.092\sqrt{c} + 0.261c)^{-4} + c^{-4}/1296]^{-1/4}$ , KCl =  $-c(0.00666 + 0.0393c^2)^{-1/4}$ , NaCl =  $-c(0.0001 + 0.00193c^2)^{-1/4}$ .

Following this line of argument, we calculated the surface potential for different salts. First, using previous equations we calculated the surface excesses of cations and anions and found surface charge as

$$Q = F(\Gamma_{\text{cation}(W)} - \Gamma_{\text{anion}(W)}) \quad (23)$$

where  $F$  is a Faraday. Using the data for the interface nitrobenzene-water,<sup>22</sup> we assumed that at low concentration the limiting value of the double layer capacitance is about 0.1 F/m<sup>2</sup>. The results for NaCl are presented in Figure 7A by the straight line marked PZ. Calculations based on the Gouy-Chapman theory, as described in the section Concentration Dependence of Surface Tension, are presented by the line marked GC.

One can see that the Parsons-Zobel effect works only at small concentrations where it predicts bigger capacitance and hence the smaller magnitude of the surface potential than Gouy-Chapman theory. Later on, this relationship changes and the Gouy-Chapman theory determines the limiting value of capacitance. Therefore the actual curve should smoothly change from PZ to GC as presented by the "Approximation" line.

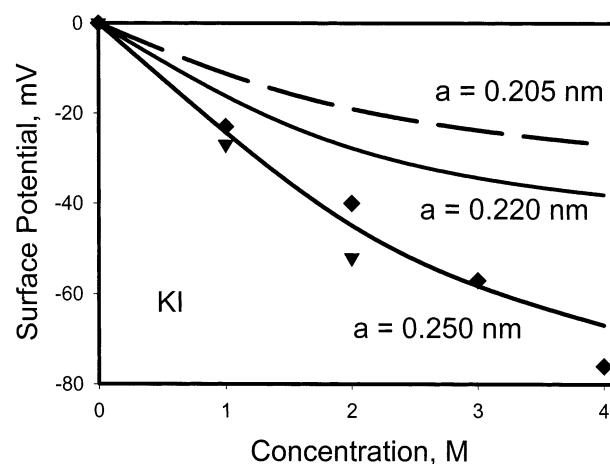


**Figure 8.** Surface potential of an aqueous solution of KI. Experimental points are taken from Frumkin<sup>8,9</sup> (▽) and Jarvis and Scheiman<sup>11</sup> (◆). The radius of I<sup>-</sup> was taken as 0.206 nm<sup>21</sup> (dashed line, equation =  $-[(18.839\sqrt{c} - 2.514c)^{-4} + c^{-4}/20736]^{-1/4}$ ), or the crystallographic radius of 0.22 nm (thin continuous line, equation =  $-[(30.42\sqrt{c} - 5.429c)^{-4} + c^{-4}/83521]^{-1/4}$ ), or estimated as 0.25 nm (solid line, equation =  $-x[2.744 \times 10^{-6} + 0.000138x^2(9.23 - 4.724c\sqrt{c})^{-4}]^{-1/4}$ ).

Similar calculations were performed for a number of salts and the results are presented in Figure 7B. Notice that the surface potential for KF is positive and all the others are negative, in total agreement with experimental data.

In Figure 8 we present data for KI. Iodide salts often display a number of peculiarities that put them aside from other simple salts of alkali metals. For example, iodide in aqueous solutions in the presence of oxygen has the tendency to form complexes such as IO<sub>3</sub><sup>-</sup> and I<sub>3</sub><sup>-</sup>. Therefore it came as no surprise that calculated curves predicted much smaller (in magnitude) surface potential than experimental data. To account for the presence of complexes I<sub>3</sub><sup>-</sup>, we took the radius of anions in this case as a fitting parameter and found that the data can be nicely described with  $r = 0.250$  nm.

## Discussion

We have calculated both surface tension and surface potential for aqueous solutions of simple electrolytes. For this purpose we used a new model of ions at the interface. It considered the solvent in the classical way as a dielectric continuum. The model took into consideration finite radii of ions, which permitted us to eliminate the divergent function, describing the energy at the interface for point ions and providing a way to distinguish between different types of ions. By applying standard methods of the electrical double layer for ions of finite radii and solving the ensuing equations, we were able to find the surface tension in a wide range of concentrations in agreement with experimental data. Previous investigations could explain the surface tension up to centimolar concentrations, and in the present work we extended this range to molar concentrations.

The surface potential was explained for the first time both qualitatively and quantitatively. The sign of the surface potential was determined by the larger ion that, in this model, was less repelled from the surface than the smaller one. However, if only the finite radii of ions were taken into account, then the calculated potentials were much smaller in amplitude than experimental data. This discrepancy happened because the surface potential is much more sensitive to the subtle details of the model than is the surface tension. Whereas the latter is determined by the sum of anion and cation adsorptions, the former is determined by their difference. This is a classical case

of a small difference of big numbers: even a very small inaccuracy of any of these big numbers brings a large error in their difference. Therefore we looked for additional effects that could help to distinguish between cations and anions. This happened to be the solvophobic effect, which does not change much the adsorption of each ion but considerably contributes to their difference. As a result, the amplitude of calculated potentials increased significantly and became closer to the observations.

Calculation of the energy of the solvophobic ion–solvent interaction is based on phenomenological or statistical mechanical molecular models in which the parameters describing both the ion and solvent are not always known. To avoid uncertainty, the solvophobic contribution to the solvation energy is sometimes estimated using the semiempirical solvophobic formula.<sup>26</sup> The main idea was formulated and discussed in a number of papers.<sup>27–31</sup>

Surface energy at the interface of cavity in water created to accommodate the ion with radius  $a$ , when expressed in terms of surface tension at the air/water interface  $\gamma_{\text{cavity}}$ , is equal to  $\Delta G^{\circ}(\text{svph}) = -4\pi a^2 \gamma$ . This relation infers that the molecules of the two solvents *water* and *air* do not mix or react chemically with each other. The hydrophobic contribution to the Gibbs free energy of ion or molecule is obviously greater for particles with larger radii,  $a$ .

One also has to take into account that ions are very small entities and the surface tension in cavities should be smaller than at the planar interface. The effect of curvature on the surface tension at a molecularly sized sphere was estimated by Tolman.<sup>20</sup> The surface tension at radius  $a$  can be written as  $\gamma_{\text{cavity}} = \gamma_{\text{planar}}(1 + 2\delta/a)^{-1}$ , where  $\delta$ , according to Tolman, is the distance from the surface of tension to the dividing surface for which the surface excess of fluid vanishes. Parameter  $\delta$  can vary between 0 and a few angstroms.<sup>20</sup> We found that this effect has optimum contribution to the adsorption of ions at  $\gamma_{\text{cavity}} = 50$  mN/m.

From a theoretical point of view, the limits of applicability of the solvophobic formula are not quite clear. Nonetheless, it works surprisingly well for calculation of the partition coefficients of a system of two immiscible liquids.<sup>32</sup>

The only problem that remained with surface potentials was the very fast growth of calculated potentials at small concentrations: they grew as a square root of concentration, meaning that it is infinitely fast, whereas experimentally potentials changed rather linearly with concentration. This last problem was resolved by taking into consideration the Parsons–Zobel effect<sup>23,24</sup> according to which at small electrolyte concentrations the capacitance of the double layer did not vary like  $\sqrt{c_0}$ , but rather became constant in an obvious contradiction with the classical point of view. We modified our calculations at small concentrations by taking into account the constant capacitance and providing the smooth transition from one limiting case to another. The results are presented in Figures 7 and 8.

So, our analysis was based on the model that accounts for finite radii of ions, the solvophobic effect and the Parsons–Zobel effect. The model worked rather nicely for simple ions such as  $\text{Na}^+$ ,  $\text{K}^+$ ,  $\text{Cl}^-$ , and  $\text{F}^-$ , as one can see in Figure 7. However, with ions having the tendency to redox and photoredox reactions with oxygen (air), like iodide that is known to form  $\text{IO}_3^-$  and  $\text{I}_3^-$  ions, the situation is different. Following the same method we have calculated the surface potential for the solution of KI, assuming the radius of  $\text{I}^-$  equal to 0.205 nm according to Gourary and Adrian<sup>21</sup> or the crystallographic value of 0.220 nm.<sup>4</sup> The theoretical curves are presented by the broken

and thin continuous lines in Figure 8. As one can see, both of them predict much smaller potential than was actually observed. We believe that it is due to the fact that a fraction of iodide ions exists in the form of  $\text{I}_3^-$  or  $\text{IO}_3^-$  complexes and has a bigger radius. We did not try to estimate its value independently but rather considered it as an effective radius and a curve-fitting parameter to achieve the agreement between the theory and experiment. We found that it can be done with an effective radius of 0.250 nm. This number does not seem unrealistic and hence it provides an estimate of an important parameter for this salt. Similar problems were encountered with KBr and  $\text{KNO}_3$  (not shown).

We found a reasonable agreement between the theory and experiment, although not an ideal one. There are a few reasons for certain discrepancies. First, the experimental data on the surface potential is not very numerous and often are contradictory. Measuring the surface potential is a rather delicate procedure and it is also method-dependent. Surface potentials at the air/water interface can be measured by the dynamic capacitor method,<sup>19</sup> the radioactive probe method,<sup>11</sup> and the jet electrode method.<sup>8,9,33</sup> Each method gives the opportunity to measure surface potential at the air/water interface with the accuracy about  $\pm 1$  mV, but difference in measured values between different authors can reach more than 10%. There can be a problem with elimination of diffusional potential in the salt bridge between the measuring cell and the reference electrode<sup>8,9</sup> or effect of charge generation by the radioactive probe. For example, for 0.5 M KI aqueous solution surface potential was measured to be equal to 22,<sup>8,9</sup> 10,<sup>12</sup> or 12 mV.<sup>11</sup>

Second, the present theory is based on a rather simple (although improved with respect to previous ones) model of interface. The early publications<sup>34,35</sup> merely assumed that there is a layer of a few water molecules at interface completely devoid of ions. This naïve approach could explain qualitatively the increments of the surface tension but was unable to explain the surface potential. For this purpose, Randles<sup>22</sup> arbitrarily postulated that this layer is accessible to only one type of ion and hence the surface potential can build up. However, even in this case results were qualitatively unsatisfactory.

Our model overcomes these difficulties. It is formulated in a classical way where the solvent is modeled as a continuum dielectric characterized by its macroscopic dielectric properties. This approach invokes a simple, easily interpretable physical picture that does not involve many adjustable parameters. However, it applies the concept of the macroscopic dielectric response to microscopic distances where it may not have a clear physical meaning.

There is a number of other aspects where our model may be vulnerable to criticism. It is obviously naïve to visualize the air/water interface as a flat and sharp dielectric border between two phases. Fluid interfaces are usually treated in electrochemistry like that, but they are known to be never ideally flat because of the thermal excitation of capillary waves. Capillary waves induce roughness of fluid interfaces and may influence their electrochemical properties.<sup>36</sup>

So, the surface is dynamic, its dielectric constant changes with distance and so on. One could not expect from this simple model to provide an ideal agreement with the experiment. It is rather surprising that we were able to go this far predicting the surface tension with a discrepancy of only about 10% and about the same for the surface potential. It is rather amazing because the model completely ignores many important properties of the system like the discrete nature of the solvent, dynamic variability of the interface, and many other features. Any future develop-



ment should include all these features and account for the detailed structure of the interface.

Unfortunately, this structure is not very well-known. There are a number of publications where authors try to elucidate the structure of water interface and the manner in which ions interact.<sup>36,37</sup> One interesting question is if the water molecules at a certain degree are oriented at the interface. If they are, then they could create a permanent dipole potential at the interface that could influence the distribution of ions at the interface and hence generate the increment of the surface potential in the presence of electrolytes.

However, opinions about this issue are controversial. There are no reliable experiments to determine this orientation. Computational methods of molecular dynamics might be helpful but different authors come to different conclusions.

Wilson and Pohorille,<sup>37</sup> as well as other authors cited in this paper, found that the molecular dipoles of water tend to lie parallel to the surface with a slight asymmetry of this distribution. This leads to a net dipole moment of the interfacial layer of water pointing to the liquid.

Wilson and Pohorille<sup>37</sup> studied ions  $\text{Na}^+$ ,  $\text{Cl}^-$ , and  $\text{F}^-$  at the water–vapor interface. They came to the rather unexpected conclusion that the free energy curves of two anions at the interface are qualitatively similar to one another, and qualitatively different from the free energy curve of the cation, which is more strongly repelled from the interface. Because  $\text{Na}^+$  and  $\text{F}^-$  are about the same size, whereas  $\text{Cl}^-$  is larger than  $\text{F}^-$ , Wilson and Pohorille concluded that the free energy required to move these simple, monovalent ions to within one molecular layer of the interface depends primarily upon the sign of their charges and not upon their sizes. They ascribed this effect to the asymmetric orientational distribution of water molecules at the pure water liquid–vapor interface. Another interesting conclusion is related to the solvation of ions at the interface. The ions at the surface were found to retain their solvation shells. As a consequence of this, a bulge is formed in the surface above the ion. The size of this bulge was found to depend more on the sign of the charge of the ions than on their relative sizes.

In the more recent paper, Marrink and Marcelja<sup>38</sup> (see also references within) presented a different picture. They claimed that water molecules near an interface tend to order themselves in such a way that configurations with hydrogens pointing outward from the liquid and oxygens inward are slightly more favorable than the other way around. This is opposite to the opinion of Wilson and Pohorille. With molecular dynamics simulation, Marrink and Marcelja<sup>38</sup> found that the water–vapor interface is rather broad so that the density of water molecules changes from the bulk value to zero at a distance of about 0.5 nm. They studied  $\text{Na}^+$  and  $\text{Cl}^-$  ions at this interface and found that the dipole moment of the surface layers of water does not influence the distribution of ions. The repulsion of ions from the interface they ascribed mainly to the decrease in water density. The ions “feel” the reduced water density and are repelled already at a large distance. The reduced density appears to affect the hydration shells of the ions. Marrink and Marcelja found that the energy curves describing sodium and chloride are very similar, but chloride ions seem to be repelled more than sodium ions (?).

This conclusion is difficult to reconcile because it contradicts experimental observations. If true, the surface potential of the NaCl solution would be positive, whereas experimentally it is very well-known to be negative.<sup>4,11,21</sup>

Therefore, at the present time, the state of molecular dynamic simulations cannot provide an unequivocal explanation of

surface potentials of aqueous solutions of electrolytes. Because of this, the conventional approach to the surface phenomena preserves its importance. This paper represents the application of classical electrostatics to the description of interfacial phenomena in a quantitative, consistent and almost fitting-free way. A few publications<sup>39,40</sup> about surface tension measurements in the presence of multivalent ions at the air/water interface appear in the literature. In the future, we plan to extend this analysis to different types of ions and interfaces.

**Acknowledgment.** This work was supported by NASA grant NAG8-1734 and by the National Science Foundation grant HRD-9908993.

## References and Notes

- (1) Volkov, A. G.; Mwesigwa, J.; Labady, A.; Kelly, S.; Thomas, D. J.; Lewis, K.; Shvetsova, T. *Plant Sci.* **2002**, *162*, 723.
- (2) Heydeweller, A. *Ann. Phys.* **1910**, *33*, 145.
- (3) Bikerman, J. J. *Physical Surfaces*; Academic Press: New York, 1970.
- (4) Lide, D. R., Ed. *CRC Handbook of Chemistry and Physics*, 77th ed.; CRC Press: New York, 1996.
- (5) Wagner, C. *Phys. Z.* **1924**, *25*, 474.
- (6) Onsager, L.; Samaras, N. N. T. *J. Chem. Phys.* **1934**, *2*, 528.
- (7) Buff, F. P.; Stillinger, F. H. *J. Phys. Chem.* **1955**, *11*, 312.
- (8) Frumkin, A. N. *Sbornik rabot po chistoy i prikladnoy khimii*; Scientific Chemical Technical Publishing House: Petrograd, 1924; pp 106–126 (in Russian).
- (9) Frumkin, A. N. *Z. Phys. Chem.* **1924**, *109*, 34.
- (10) Suggitt, R. M.; Aziz, P. M.; Wetmore, F. E. W. *J. Am. Chem. Soc.* **1949**, *71*, 676.
- (11) Jarvis, N. L.; Scheiman, M. A. *J. Phys. Chem.* **1968**, *72*, 74.
- (12) Randles, J. E. B. In *Advances in Electrochemistry and Electrochemical Engineering*; Delahay, P., Ed.; Interscience: New York, 1963; Vol. 3, pp 1–30.
- (13) Krylov, V. S.; Levich, V. G. *Dokl. Acad. Nauk SSSR* **1964**, *159*, 409.
- (14) Levin, Y. *J. Chem. Phys.* **2000**, *113*, 9722.
- (15) Kharkats, Yu.; Ulstrup J. *J. Electroanal. Chem.* **1991**, *308*, 17.
- (16) Ulstrup J.; Kharkats, Yu. I. *Russ. J. Electrochem.* **1993**, *29*, 299.
- (17) Wu, K.; Jedema, M. J.; Schenter, G. K.; Cowin, J. P. *J. Phys. Chem. B* **2001**, *105*, 2483.
- (18) Benjamin, I. *Annu. Rev. Phys. Chem.* **1997**, *48*, 407.
- (19) Volkov, A. G.; Deamer, D. W.; Tanelian, D. I.; Markin, V. S. *Liquid Interfaces in Chemistry and Biology*; J. Wiley: New York, 1998.
- (20) Tolman, R. C. *J. Chem. Phys.* **1949**, *17*, 333.
- (21) Gourary, B. S.; Adrian, F. S. *Solid State Phys.* **1960**, *10*, 127.
- (22) Randles, J. E. B. *Discuss. Faraday Soc.* **1957**, *24*, 194.
- (23) Samec, Z.; Marecek, V.; Homolka, D. *J. Electroanal. Chem.* **1985**, *187*, 31.
- (24) Wandlowski, T.; Holub, K.; Marecek, V.; Samec, Z. *Electrochim. Acta* **1995**, *40*, 2887.
- (25) Volkov, A. G.; Deamer, D. W.; Tanelian, D. I.; Markin V. S. *Prog. Surf. Sci.* **1996**, *53*, 1.
- (26) Kornyshev, A. A.; Volkov, A. G. *J. Electroanal. Chem.* **1984**, *180*, 363.
- (27) Sisskind, B.; Kasarnowsky, J. *Zh. Fiz. Khim.* **1933**, *4*, 683.
- (28) Uhlig, H. H. *J. Phys. Chem.* **1937**, *41*, 1215.
- (29) Markin, V. S.; Volkov, A. G. *J. Electroanal. Chem.* **1987**, *235*, 23.
- (30) Bartell, L. S. *J. Phys. Chem. B* **2001**, *105*, 11615.
- (31) Bykov, T. V.; Zeng, X. C. *J. Phys. Chem. B* **2001**, *105*, 11586.
- (32) Markin, V. S.; Volkov, A. G. *Electrochim. Acta* **1989**, *34*, 93.
- (33) Kochurova, N. N.; Dement'ev, S. Yu.; Rusanov, A. I. *Russ J. Appl. Chem.* **1977**, *70*, 657.
- (34) Harkins, W. D.; Gilbert, E. C. *J. Am. Chem. Soc.* **1926**, *48*, 604.
- (35) Harkins, W. D.; McLaughlin, H. M. *J. Am. Chem. Soc.* **1925**, *47*, 2083.
- (36) Daikhin, L. I.; Kornyshev, A. A.; Urbakh, M. *J. Electroanal. Chem.* **2000**, *483*, 68.
- (37) Wilson, M.; Pohorille, A. *J. Chem. Phys.* **1991**, *95*, 6005.
- (38) Marrink, S.-J.; Marcelja, S. *Langmuir* **2001**, *17*, 7929.
- (39) Matubayasi, N.; Matsuo, H.; Yamamoto, K.; Yamaguchi, S.; Matuzawa, A. *J. Colloid Interface Sci.* **1998**, *209*, 398.
- (40) Weissenborn, P. K.; Pugh, R. J. *J. Colloid Interface Sci.* **1996**, *184*, 550.